Available online at www.sciencedirect.com
ScienceDirect
Materials Science and Engineering C 28 (2008) 826–830
MATERIALS SCIENCE & ENGINEERING C
www.elsevier.com/locate/msec

Functionalization of niobium electrodes for the construction of impedimetric biosensors

S. Helali [a,*], A. Abdelghani [a], I. Hafaiedh [a], C. Martelet [b], M.I. Prodromidis [c], T. Albanis [c], N. Jaffrezic-Renault [d]

[a] *Unité de recherche de Physique des Semiconducteurs et Capteurs, IPEST, La Marsa, Tunisia*
[b] *Centre de Génie Electrique de Lyon, CEGELY, ECL, 69134 Ecully cedex, France*
[c] *Department of chemistry, University of Ioannina, 45110 Ioannina, Greece*
[d] *Laboratoire des Sciences Analytiques, CNRS UMR 5180, Batiment Raulin, Université de Claude Bernard, 69622 Villeurbanne Cedex, France*

Available online 18 October 2007

Abstract

This paper describes the development of an impedimetric immunosensor, based on niobium/niobium oxide (Nb/NbOxHy) electrodes, for the detection of atrazine. Niobium oxide was anodically formed onto niobium electrodes at 25 V in 1 M H_2SO_4. Hydrous oxide layers were then silanized with APTES, and using glutaraldehyde as a cross linker, Fab fragment k47 antibody was covalently immobilized onto the surface of the electrodes. Electrochemical impedance spectroscopy (EIS) was used to characterize the building-up of the immunosensors as well as the binding of atrazine to its specific antibody. In presence of ferricyanide redox species and under a cathodic polarization voltage (−1.2 V *versus* SCE), the relationship between the concentration of atrazine and the change of the electron transfer resistance value was studied.
© 2007 Elsevier B.V. All rights reserved.

Keywords: Atrazine; Niobium electrode; Anodic niobium oxide; Electrochemical impedance spectroscopy; Biosensors

1. Introduction

Electrochemical immunosensors have found widespread applications in food industry, environment, biotechnology, pharmaceutical chemistry and clinical diagnostics [1–3]. Important analytical characteristics, such as high sensitivity and specificity, cost efficiency, and their ability to be used as disposable sensors for in-field measurements make them promising alternatives to conventional immunoassay techniques. Among other sensing approaches, which are based on potentiometric [4,5], amperometric [6] and piezoelectric [7,8] transducers, electrochemical impedance spectroscopy (EIS) provides a non-destructive means for the characterization of the electrical properties of many biological interfaces. In recent years the electrochemical impedance immunosensors have attracted increasing interest for the direct monitoring of the formation of antigen-antibody complex [9–12], biotin–avidin complexes [13–16] and DNA hybridization [17]. However, antigen–antibody is often inadequate to generate a highly sensitive signal through direct impedimetric measurement. A key step in the construction of an impedimetric biosensor is the development of the insulating layer. It should be compact, smooth, stable over time in the tested electrolyte and provide functional groups for the immobilization of the bioreceptor. An initial high capacitance (low impedance) is also a prerequisite for achieving better sensitivity and wider dynamic range [18]. Recently, a significant progress has been made in the preparation of new classes of niobium oxide surfaces [19–22] whose dielectric constant is in the order of forty leading to a high capacitance. Niobium is a refractory metal that conducts heat and electricity and is characterized by a resistance to corrosion. It is world-wide used mostly in the steel industry, the industry of super alloys and the industrial sectors that use oxides and other Nb based compounds for the manufacture of optical glasses and enamels. The present work explores the use of anodically formed niobium/niobium oxide electrodes for the construction of an impedimetric immunosensor. The alteration of the interfacial features of the electrodes, due to different modification or recognition steps, was traced by faradaic electrochemical

* Corresponding author. Tel.: +216 71 740 048; fax: +216 71 746 551.
E-mail address: salwahleli@yahoo.fr (S. Helali).

0928-4931/$ - see front matter © 2007 Elsevier B.V. All rights reserved.
doi:10.1016/j.msec.2007.10.078

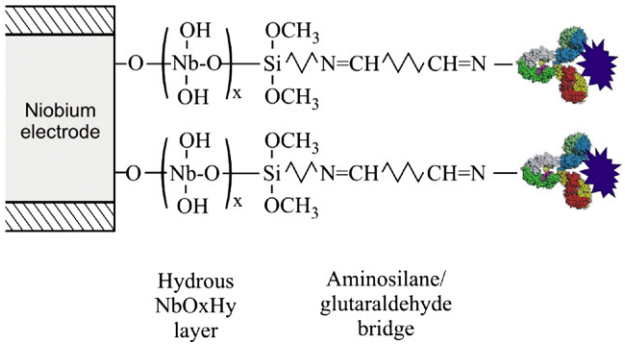

Fig. 1. Schematic diagram of the stepwise assembly of niobium electrode.

impedance spectroscopy using a mixture of hexacyanoferrate (II)/(III), as a redox probe.

2. Experimental

2.1. Materials

Atrazine was purchased from SUPELCO (Bellefonte, USA). The antibody Fab fragment K47 was obtained from Technische Universitat Munchen, Germany. γ-amino propyl-trimethoxy silane (APTES), and glutaraldehyde (grade II, 25%) were obtained from Sigma (St. Louis, USA) and used as received. All measurements were made in a phosphate buffered saline (PBS) containing 140 mM NaCl, 2.7 mM KCl, 0.1 mM Na_2HPO_4, 1.8 mM KH_2PO_4, pH = 7 and 5 mM $K_3[Fe(CN)_6]/K_4[Fe(CN)_6]$ (1:1) mixture as a redox probe. All reagents were of analytical grade and ultrapure water (resistance 18.2 MΩ cm^{-1}) produced by a Millipore Milli-Q system was used throughout.

2.2. Apparatus

The measurement set-up for impedance consists of a classical three-electrode electrochemical cell, that was placed into a Faraday cage. The modified niobium/niobium oxide electrode (0.03 cm^2) was used as working electrode, a platinum strip (0.54 cm^2) as a counter electrode and a saturated calomel electrode (SCE) as the reference electrode. The impedance analysis was performed with the Voltalab 40 impedance analyser in the frequency range 0.05–100 kHz, using a modulation voltage of 10 mV. During measurements the potential was kept at −1.2 V versus SCE. Data simulation was made with the commercial software Zview (Scribrer and associates,

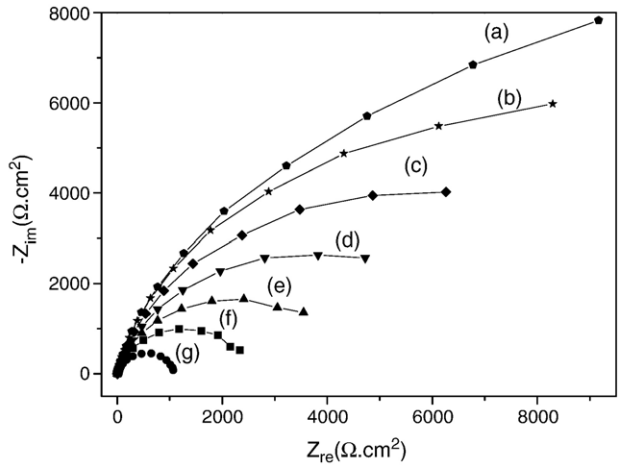

Fig. 2. Electrochemical impedance spectra for niobium electrode functionalized by silane after apply potential: (a)− 0.6, (b) − 0.7, (c) − 0.8, (d) 0.9, (e) 1, (f) − 1.1 and (g) − 1.2 V.

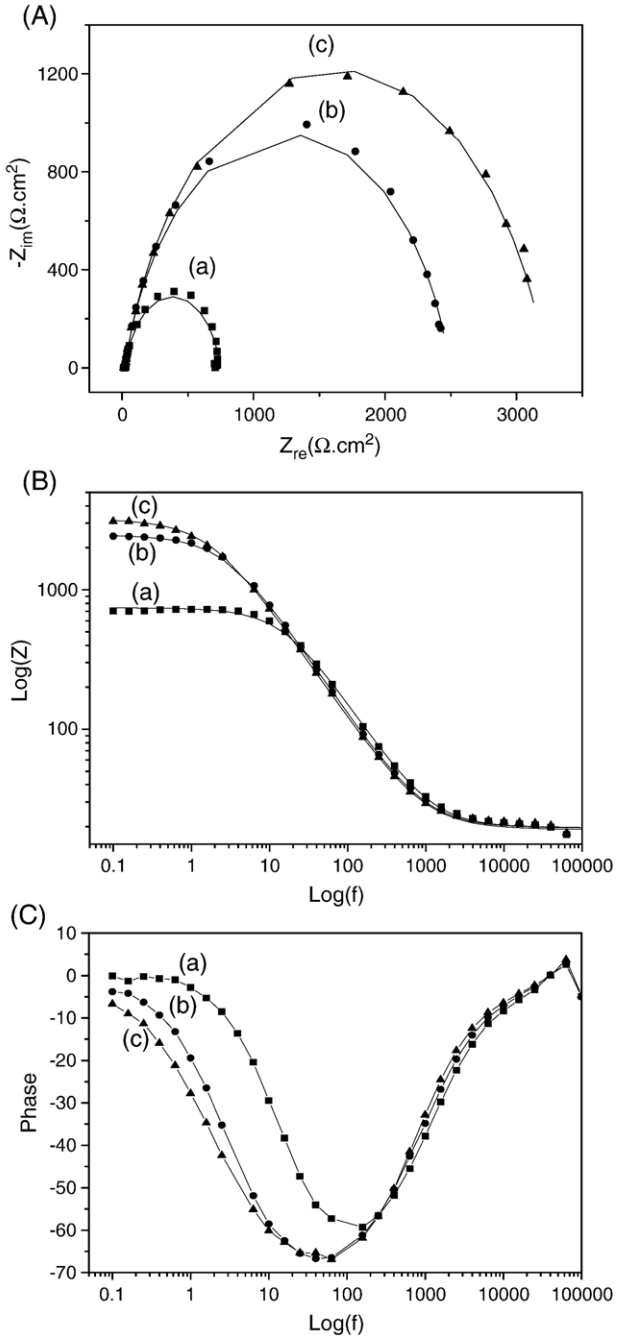

Fig. 3. (A) Nyquist and (B,C) Bode plots of electrochemical impedance spectra: (curve a) Nb/NbOxHy/aminosilane, (curve b) Nb/NbOxHy/aminosilane/glutaraldehyde, and c) Nb/NbOxHy/aminosilane/glutaraldehyde/fab fragment k47 antibody electrodes at −1200 mV over the frequency range 0.05–10^5 Hz in 5 mM $K_3[Fe(CN)_6]/K_4[Fe(CN)_6]$ in PBS pH 7.

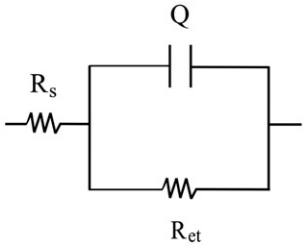

Fig. 4. Equivalent circuit employed for all data fits.

Charlottesville, VA). All electrochemical measurements were carried out at room temperature.

2.3. Electrode fabrication and modification

Niobium electrodes of 2 mm diameter active surface were fabricated by using the commercial kit EasyCon (EasyCon Hellas, provided by Eco Chemie). Niobium disks (0.5 mm thick, 2 mm diameter) were glued on a bronze rod (2 mm diameter) with the aid of a silver-based conductive adhesive. A two-component epoxy resin was used to ensure no electrical contact between the conductive adhesive and the bronze rod with the electrolyte. Niobium electrodes were further covered with 4 and 6 mm diameter heat-shrink tubing. Before use, niobium electrodes were polished with a series of emery papers (400, 1200, 2000 and 4000 grit), sonicated for 3 min in DDW, and then etched in a $H_2O_2/H_2SO_4/H_2O$ (1/1/5) mixture for 2 min. Passive films of niobium oxide were anodically formed at 25 V in 1 M H_2SO_4 for 1 h. Films were then silanized in 10% APTES (*Note*: Handling must be carried out in a hood wearing rubber gloves) in chloroform for 2 h. The silanized surfaces were activated with 2.5% glutaraldehyde for 1 h in the working buffer solution. Functionalized electrodes were immersed in 5 ml PBS, pH 7 with 2.6×10^{-7} M of Fab fragment K47H antibody at room temperature for 1 h and then thoroughly rinsed with PBS to remove weakly absorbed antibodies. Finally, electrodes were exposed to various concentrations of atrazine and alteration of the interfacial properties of the electrodes upon antigen–antibody interaction was recoded and discussed (Fig. 1).

3. Results and discussions

3.1. Polarization potential

The influence of the applied potential on EIS response was investigated and the results are shown in Fig. 2. As revealed from the pattern of impedance spectra, the Warburg impedance resulting from the diffusion process is gradually decreased upon the increase of the applied cathodic polarization potential. At −1.2 V vs SCE, the effect of Warburg impedance was neglected and the impedance spectra presented the best semi-circle like shape. Therefore, −1.2 V vs SCE was proved as the suitable polarisation potential for subsequent impedimetric studies.

Table 1
Values of circuit elements obtained by fitting experimental data from Fig. 3 to the discrete circuit model shown in Fig. 4

Electrodes	R_s (Ω cm^2)	R_{et} (Ω cm^2)	Q (μF/cm^2)	α
Silane	19.68	725.7	0.26	0.85
Glutaraldehyde	19.53	2470	0.36	0.83
Ac	19.05	3209	0.41	0.82

Table 2
Changes of R_{et} after the incubation of Nb/NbOxHy/silane/glutaraldehyde/fab fragment k47 antibody electrodes at different concentrations of atrazine, resulted from fitting the experimental data from Fig. 5A with the equivalent circuit in Fig. 4

Concentration of atrazine (μg/ml)	R_{et} (Ω cm^2)	ΔR_{et}(Ω cm^2)
100	3752	543
200	5472	2263
500	5653	2444
700	5864	2655

3.2. Electrochemical characterization of the sensor

Anodization studies aim the development of a smooth, homogenous and compact oxide layer. Nb/NbOxHy electrodes were developed at different applied potentials up to 30 V versus

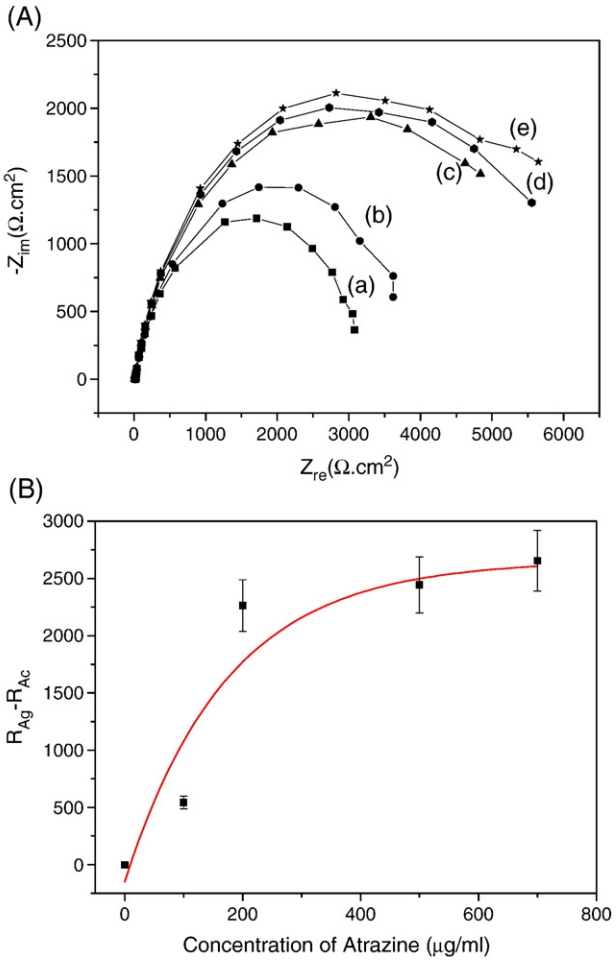

Fig. 5. (A) Electrochemical impedance spectra of immunosensor response after the addition of different concentrations of antigen: (a) without antigen, with (b) 100 μg/ml, (c) 200 μg/ml, (d) 500 μg/ml and (e) 700 mg/ml of antigen. Experimental conditions as in Fig. 3. (B) R_{et} change as a function of the concentration of atrazine.

SCE, and the stability of them in PBS, a very common buffering system in bioanalytical studies, was studied. Electrodes were found to be sensitive to PBS buffer solution, since the measuring impedance of them was gradually decreasing with respect to time, probably due to pitting corrosion of chloride ions. The formation potential of 25 V versus SCE was finally selected, as under these conditions we achieved the best reproducible electrode architectures in terms of their impedance values in the working buffer solution. A remarkable increase of the stability of the electrodes was observed after their silanization with APTES. An increased coverage of amino-silane, over the hydroxylated Nb/NbOxHy surface was found to protect the latter from pitting corrosion, thus providing a stable oxide-silane composite surface. Moreover, the particular silane bears proper functional end groups, *i.e.* $-NH_2$ groups, which are necessary for the immobilization of the sensing biolayer. The impedimetric behaviour of partially constructed and fully functionalized Nb/NbOxHy/aminosilane/glutaraldehyde/antibody electrodes is shown in Fig. 3. Faradaic impedimetric data are presented in the form of both Nyquist and Bode plots and provide a clear view of the effect of each modification step on the impedance and phase values over the entire tested frequency range.

Impedance spectra consisted of a semicircle corresponding to an electron transfer limiting process. The diameter of the semicircle representing the electron-transfer resistance (R_{et}) of each layer, is closely connected with the hindering of the flux of the redox couple towards the surface of the electrode and can be used to describe the interface properties of the electrode. Indeed, the increase of its value after each step gives evidence for the successful application of each layer.

Best fitting of the impedance data, over the entire tested frequency range were obtained by using the modified Randle's equivalent circuit [23,24], shown in Fig. 4. The proposed circuit includes the following three elements: (i) the ohmic resistance of the electrolyte solution, R_s; (ii) a constant phase element Q, which is associated with the double layer and reflects the interface between the assembled film and the electrolyte solution [25]; and (iii) the electron transfer resistance, R_{et} [26,27]. A negligible change in R_s was observed during the deposition of the aminosilane layer, during the activation of amino groups with glutaraldehyde, and finally, during the immobilization of the antibody. On the other hand, Q and R_{et}, which represent the interfacial properties of electrode/electrolyte are greatly affected during the building-up of the biolayer on the Nb electrode. Results shown in Table 1 indicate that signal changes of R_{et} are significantly higher compared to those observed for Q. Therefore, the change of R_{et} values is chosen as a measure for tracing the interaction between the fully functionalized electrode and atrazine. The fitting values for the stepwise-assembled layers on the electrode are presented in Table 1.

3.3. Application to atrazine standard solutions

To evaluate the reaction between Fab fragment k47 antibody and atrazine, Nb/NbOxHy/aminosilane/glutaraldehyde/antibody electrodes were exposed to different concentrations of atrazine. The corresponding impedance spectra (Nyquist plots) are shown in Fig. 5A, and the fitting values of R_{et} are presented in Table 2. In all cases a significant increase of the R_{et} value was observed, due to the binding of atrazine molecules to the immobilized Fab fragment k47 antibody. Fig. 5B shows the calibration plot obtained for the atrazine assay. The impedance increment is defined as:

$$\Delta R_{et} = R_{Ag} - R_{Ab}$$

where R_{Ag} is the value of R_{et}, after the immunoreaction and R_{Ac}, the value of R_{et} obtained for the fully functionalized electrode. As it can be seen in Fig. 6, quantification of the analyte concentration with the above-mentioned parameters is possible and an almost linear relationship up to 300 μg/ml atrazine can be achieved. Under the specific experimental conditions and for a signal-to-noise ratio of 3, the detection limit was calculated to be 50 μg/ml atrazine.

4. Conclusion

This study was led on functional immunosensors, based on Fab fragment k47 antibody grafted on Nb/NbO_2 electrodes. Impedance spectroscopy was successfully applied for the direct monitoring of antibody-antigen interactions, using an hexanocyanoferrate(II)/(III) mixture as a redox probe, allowing detection of atrazine at concentration level of as low as 50 μg/ml.

Acknowledgements

This work is financially supported by NATO through CBP. MD.CLG.982802 Collaborative Linkage Grant. The financial support of EC (Project IMAGEMO; QLK3-CT-2002-02141) is gratefully acknowledged. The authors thanks the Alexander Von Humboldt (Germany) for the material donation.

References

[1] H. Chen, J. Jiang, Y. Huang, T. Deng, Ji. Li, Gu. Shen, Ru. Yu, Sens. Actuators, B, Chem 117 (2006) 211.
[2] C.A. Rowe, S.B. Scruggs, M.J. Feldstein, J.P. Golden, F.S. Ligler, Anal. Chem. 71 (1999) 433.
[3] M.A. Gonźalez-Martínez, R. Puchades, A. Maquieira, Trends Anal. Chem. 18 (1999) 204.
[4] S. Gracheva, C. Livingstone, J. Davis, Anal. Chem. 76 (2004) 3833.
[5] S.Q. Hu, Z.Y. Wu, Y.M. Zhou, Z.X. Cao, G.Li. Shen, R.Q. Yu, Anal. Chim. Acta 458 (2002) 297.
[6] A.K. Singh, P.K. Kilpatrick, R.G., Biotechnol.Prog 11 (1995) 333.
[7] G. Shen, S. Tan, H. Nie, G. Shen, R. Yu, J. Immunol. Methods 313 (2006) 11.
[8] A. Tlili, A. Abdelghani, S. Hleli, M.A. Maaref, Sensors 4 (2004) 105.
[9] F. Darain, D.S. Park, Y.B. Shim, Biosens. Bioelectron. 19 (2003) 773.
[10] M. Wang, L. Wang, G. Wang, X. Ji, Y. Bai, T. Li, S. Gong, J. Li, Biosens. Bioelectron. 19 (2003) 575.
[11] X. Cui, D. Jiang, P. Diao, J. Li, R. Tong, X. Wang, J. ElectroAnal. Chem. 470 (1999) 9.
[12] I. Navrátilová, P. Skládal, Bioelectrochemistry. 62 (2004) 11.
[13] S. Helali, C. Martelet, A. Abdelghani, F. Bessueille, A. Errachid, J. Samitier, H.C.W. Hays, P.A. Millner, N. Burais, N. Jaffrezic-Renault, Mater. Sci. Eng., C, Biomim. Mater., Sens. Syst. 26 (2006) 322.
[14] S. Helali, C. Martelet, A. Abdelghani, N. Burais, N. Jaffrezic-Renault, Sens. Actuators, B, Chem 113 (2006) 711.

[15] J. Minic, J. Grosclaude, J. Aioun, M.A. Persuy, T. Gorojankina, R. Salesse, E. Pajot-Augy, Y. Hou, S. Helali, N. Jaffrezic-Renault, et al., Biochim. Biophys. Acta 27 (2006) 576.
[16] Y. Hou, S. Helali, A. Zhang, N. Jaffrezic-Renault, C. Martelet, J. Minic, T. Gorojankina, M.A. Persuy, E. Pajot-Augy, R. Salesse, et al., Biosens. Bioelectron. 21 (2006) 1393.
[17] S. Hleli, A. Abdelghani, A. Tlili, Sensors 3 (2003) 472.
[18] A. Gebbert, M. Alvarez-Icaza, W. Stocklein, R.D. Schmid, Anal. Chem. 64 (1992) 997.
[19] K. Schumacher, M. Grun, K.K. Unger, Microporous Mesoporous Mater. 27 (1999) 201.
[20] I. Nowak, Stud. Surf. Sci. Catal. 142 (2002) 1363.
[21] X.T. Gao, I.E. Wachs, M.S. Wong, J.Y. Ying, J. Catal. 203 (2001) 18.
[22] V. Parvulescu, C. Anastasescu, C. Constantin, B.L. Su, Catal. Today 78 (2003) 477.
[23] Wiegand, Ph.D thesis: Fundamental principles of the electric properties of supported lipid membranes investigated by advanced methods of impedance spectroscopy, 1999, Shaker Verlag, ISBN 3-8265-7231-9, Technishe Universitat of Muenchen, Germany.
[24] H. Huang, Z. Liu, X. Yang, Anal. Biochem. 356 (2006) 208.
[25] S. Helali, C. Martelet, A. Abdelghani, M.A. Maaref, N. Jaffrezic-Renault, Electrochim. Acta 51 (2006) 5182.
[26] A.J. Bard, L.R. Faulkner, Electrochemical Methods: Fundamentals and Applications, second ed. John Wiley, New York, 2000.
[27] L. Yang, Y. Li, Biosens. Bioelectron. 20 (2005) 1407.